

## Tribology in Industry

[www.tribology.fink.rs](http://www.tribology.fink.rs)

# Dry Sliding Wear Behavior of A356 Alloy/Mg<sub>2</sub>Si<sub>p</sub> Functionally Graded in-situ Composites: Effect of Processing Conditions

S.C. Ram<sup>a</sup>, K. Chattopadhyay<sup>a</sup>, I. Chakrabarty<sup>a</sup>

<sup>a</sup>Department of Metallurgical Engineering, IIT(BHU), Varanasi, UP, India-221005.

---

### Keywords:

FGMs  
MMCs  
A356 alloy/Mg<sub>2</sub>Si<sub>p</sub> in-situ composites  
Dry sliding wear  
Centrifugal casting

---

### Corresponding author:

S.C. Ram  
Department of Metallurgical  
Engineering, IIT (BHU),  
Varanasi, UP,  
India-221005.  
E-mail: subh.mtech07@yahoo.com

---

### A B S T R A C T

In present study, the effect of dry sliding wear conditions of A356 alloy/Mg<sub>2</sub>Si<sub>p</sub> functionally graded in-situ composites developed by centrifugal casting method has been studied. A pure commercial A356 alloy (Al-7.5Si-0.3Mg) was selected to be the matrix of the composites and primary Mg<sub>2</sub>Si<sub>p</sub> reinforcing particles were formed by in-situ chemical reaction with an average grain size of 40-47.8  $\mu$ m. The Al-(Mg<sub>2</sub>Si)<sub>p</sub> functionally graded metal matrix composites (FGMMC's) were synthesized by centrifugal casting technique with radial geometry, using two different mould rotating speeds (1200 and 1600 rpm). The X-ray diffraction (XRD) characterization technique was carried out to confirm the in-situ formed Mg<sub>2</sub>Si particles in composites. Optical microscopy examination was carried out to reveals the grain refinement of Al-rich grains due to in-situ formed Mg<sub>2</sub>Si particles. Scanning electron microscope (SEM) and Energy dispersive X-ray spectroscopy (EDS) techniques were carried out to reveal the distribution of phases, morphological characteristics and confirmation of primary Mg<sub>2</sub>Si particles in the matrix. The sliding wear behavior was studied using a Pin-on-Disc set-up machine with sliding wear parameters: effect of loads (N), effect of sliding distances (m) and effect of Mg on wear at room temperature with a high-carbon chromium steel disc (HRC-64) as counter surfaces. A good correlation was evidenced between the dry sliding behaviour of functionally graded in-situ composites and the distribution of Mg<sub>2</sub>Si reinforcing particles. Beside the above processing conditions, the dominant wear mechanisms of functionally graded in-situ composites have been correlated with the microstructures. The hardness and wear resistance properties of these composites increase with increasing volume percent of reinforced primary Si/Mg<sub>2</sub>Si particles toward inner zone of cast cylindrical shapes. The objective of this works was to study the tribological characteristics under dry sliding conditions of fabricated composites for automotives engine blocks and cylinder liners.

---

© 2016 Published by Faculty of Engineering

## 1. INTRODUCTION

Commercially pure Al-Si alloys are rapidly being progressive demands used in the automotive and aerospace industry; especially for engine block and cylinder liners since weight reduction, improves fuel efficiency and minimizes CO<sub>2</sub> emissions. However, the pure commercially available aluminum as-cast alloys are exhibit some limitations in terms of lower the wear resistances characteristics and mechanical strength [1-2]. The major problems are having with engine liners and blocks are failure of materials used due to relative surface contact between two components resulting abrasion and wear. This process is attributed to a several factors. First, the hard phase particles presence and cooling and lubrication used, results in abrasive and corrosive wear are occurred. Second, erosive wear is also significant from the impact of hot gases and air. Third, friction between engine block wall and piston ring can produce adhesion even in oil lubrication. Finally, fatigue behavior also contributes to the wear of engine block and liners [3-4].

In considerations of above problems, the many researchers are focused to develop the FGMs with different alloying elements. Therefore, the development of functionally graded materials (FGMs) based on the Al-Mg-Si or Al-Si-Mg systems have been attracting attention in recent years, because of their gradient properties, thermal stability, functional performance and high strength to weight ratio.

In the case of Al-Mg-Si system, the formation of Mg<sub>2</sub>Si is an important strengthening phase; the many researchers had worked and established Al-Mg<sub>2</sub>Si system using different synthesis techniques. Amongst the various fabrication techniques, the centrifugal casting route is very crucial in development of functionally graded in-situ composites. However, the presence of primary Mg<sub>2</sub>Si particles in the aluminum metal matrix could lead to poor mechanical as well as wear resistance properties of fabricated composites. In order to enhance the mechanical and wear properties of functionally graded Al-Mg<sub>2</sub>Si composites, modifying or refining the structure of Mg<sub>2</sub>Si by adding different chemical elements, such as Y, Cr ,Na, Li and P, have been investigated by several researchers [5-7].

In general, as a major reinforcing phase (e.g. SiC, TiB<sub>2</sub>, ZrB<sub>2</sub>, Mg<sub>2</sub>Si and other ceramic phases), in order to reduction in weight, the Mg<sub>2</sub>Si is most effective reinforcing phase for engine block applications. In situ formed Mg<sub>2</sub>Si phase in matrix are new aspect, because of it is more capable to migrate into inner surfaces of cylindrical cast tubes due to their lighter density (1.99 gm/cm<sup>3</sup>) than Al-matrix (2.27 gm/cm<sup>3</sup>).The migration of Mg<sub>2</sub>Si particles are clearly showed into inner core of cylindrical cast tubes due to the action of centrifugal force. It is therefore desirable to understand the effect of rotational speed of mold with excess Mg addition on the microstructure and wear properties of Al-Mg<sub>2</sub>Si alloys processed by centrifugal casting [8-9].

Zhai et al. [10] have fabricated the FGMs based on Al-Si-Mg system using centrifugal casting technique, and they were found that, most of Si and Mg<sub>2</sub>Si primary crystal particles formed by in-situ reaction in the alloys. These particles were segregated and enriched in the inner layer of castings due to their smaller densities ( $\rho_{\text{Si}} = 2.33 \text{ g/cm}^3$ ,  $\rho_{\text{Mg}_2\text{Si}} = 1.99 \text{ g/cm}^3$ ) than that of Al melt ( $\rho_{\text{Al}} = 2.37 \text{ g/cm}^3$ ). Moreover, the FGMs composites were produced in two categories: stir-casting and centrifugal casting. Stir-casting process was used to produce homogeneous metal matrix composites (MMCs). Centrifugal casting (centrifugal in-situ method) was used to process the FGM's, with smoothly varying gradient properties. The FGMs formed by centrifugal casting generally shows a sudden change of appearance and is obviously divided into two layers, the particle reinforcement layer and the un-reinforcement layer with few particles.

The in-situ formed primary Si and Mg<sub>2</sub>Si particles are segregated in the reinforcement layer imparts a superior wear resistance to of the cast components. Lin et al. [11] have investigated the influences of microstructure characteristics due to Si and Mg contents of the Al-Mg<sub>2</sub>Si FGMs fabricated by centrifugal casting. Due to the presence of Si and Mg in alloys had a great effect on the formation and segregation of particles, and proper contents of Si and Mg in the alloy were provided the good refinements of grains. However, the effect of particles distribution into core with varying processing conditions, and compositions are clearly not reported yet, which are very crucial for automotive engine blocks and liners.

In accordance of the wear mechanisms, delamination, formation of a stable mechanically mixed layer (MML), oxidative wear and also two- or three-body abrasive wear are reported [12-15,18]. A high number of works refer the formation of MML as the main wear mechanism, which usually results in a mild wear regime [9-14,18,19]. Some time, the wear resistance properties of the composite materials can also be protected by MML layers because of, it also act as protective layers during wear test. Although, according to some researcher, MML are mainly constituted by material transferred from the counter surfaces which is subsequently formed the mixed layer but exact structure/composition of these layers is still under investigation [12-14,18]. Li and Tandon [19] investigated the nature of MML's formed during the dry sliding wear processes of an Al-Si composite reinforced with Mg<sub>2</sub>Si particles, using hardened chromium steel as counter surface, and reported that both the morphology and presence of the MML were dependent on the several sliding conditions.

In present investigation, a valuable work is made to study and analyze the wear failure mechanism of functionally graded Al-Mg<sub>2</sub>Si in-situ composites with varying dry sliding conditions at room temperature. Generally, at the inner surface of engine blocks and liner is required high hardness and high wear characteristics because of relative contact of wall and piston. So, due to gradient distribution of hard primary phase Mg<sub>2</sub>Si into inner core of centrifugally cast FGMs has great potential to enhance the wear properties into inner surfaces of engine blocks.

## 2. EXPERIMENTAL PROCEDURES

Commercially pure aluminium-silicon alloy (Al-7.5Si-0.3Mg) was used as starting material for melting and preparation of Al-Mg<sub>2</sub>Si functionally graded in situ composites. Firstly, three ingots of 0.30 % Mg, 10 % Mg and 20 % Mg master alloy were prepared with addition of pure Mg-turnings in required proportions. The required amount of Mg-turnings about 15 % of additional pure Mg (wrapped in the Al foil) was added to the molten master alloys in order to recover the melting loss of Mg. After that, the master alloy ingot was remelted at 800 °C in the electrical resistance furnace for 60 minutes and the MgCl<sub>2</sub>.6H<sub>2</sub>O and

KCl fluxes was added to molten alloy to avoid the loss of Mg and protect from oxidation. After completion of reaction time the Mg<sub>2</sub>Si particles are introduced into molten alloy and pouring was done with two rotation speed of mold for base A356 alloy at 1200 rpm and for others two composites at 1200 & 1600 rpm respectively. Finally, the three cylindrical casting tubes were obtained with recovery of different weight percentage of magnesium (a) as base alloy 0.30Mg and two FGMs tubes with (b) 5wt.%Mg (c) 10wt.%Mg respectively. Chemical compositions of prepared composites have been shown in Table 1.

**Table 1.** Chemical composition of alloys/FGMs.

Alloy/composites	Chemical composition [%]				
	Si	Mg	Cu	Fe	Al
A356 Alloy	7.50	0.30	0.60	1.40	Bal.
A356+5.0Mg composite	4.48	5.13	2.63	0.01	Bal.
A356+10.0Mg Composite	5.54	10.5	3.36	0.77	Bal.

The photographs of working principles of vertical centrifugal casting set-up and prepared composites have been shown in Figs. 1 and 2 respectively.

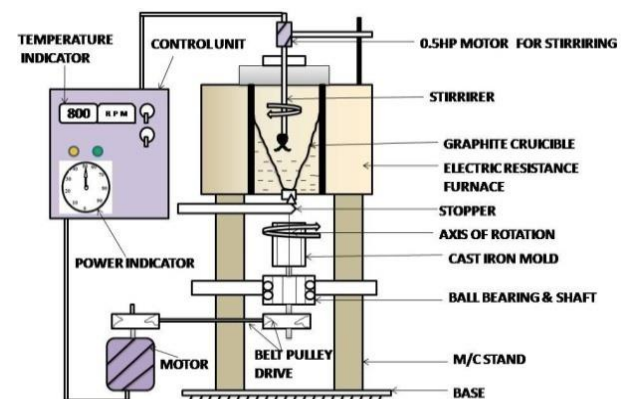


**Fig. 1.** Schematic illustration of the centrifugal casting process set-up.

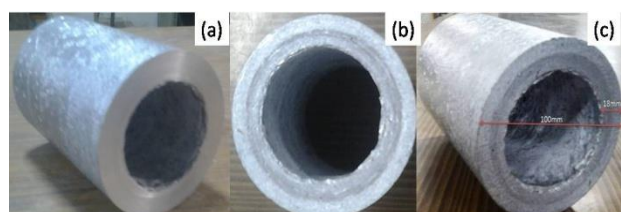


**Fig. 2.** Centrifugally cast Alloy/FGMs obtained as (a) A356 Alloy, (b) A356+5.0Mg processed at 1200 rpm and (c) A356+10.0Mg processed at 1600 rpm.

The schematic representation of cross-sectional view of centrifugally cast tubes has been presented as shown in Fig. 3. The microstructures, hardness and wear resistance properties of the centrifugally cast tubes were carried out at three zone indicated as  $Z_1$ (inner zone),  $Z_2$ (Middle zone),  $Z_3$ (outer zone) respectively..

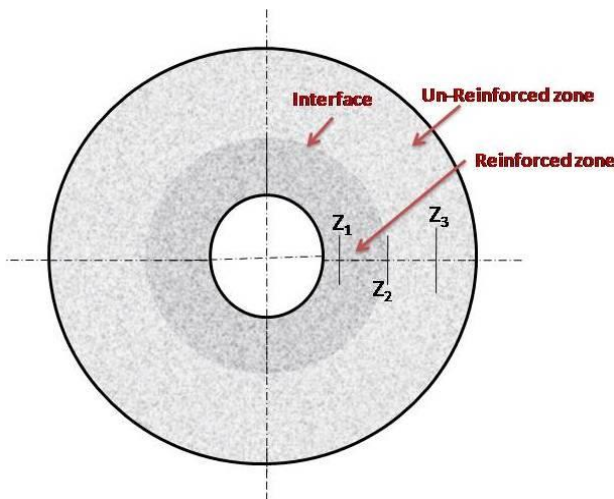


**Fig. 3.** Schematic representation of the different zones characterized from the geometrical centre of the sample: ( $Z_1=40$  mm, ( $Z_2= 46$  mm) and ( $Z_3=50.5$  mm).

XRD (Rigaku) study was carried out for identification of primary phase  $Mg_2Si/Si$  particles in composites using Cu K $\alpha$  radiation of wavelength 1.541836 $\text{\AA}$  with Ni filter. Surface morphology, phase identification and distribution of in-situ formed  $Mg_2Si$  particles were examined under SEM (FESEM Quanta 200FEG) equipped with EDS. Hardness of the base alloy and composites was estimated by Vickers Hardness Tester(LIECA) at 500 Kgf loads at three zone  $Z_1$ ,  $Z_2$  and  $Z_3$  for each composites.

A pin-on-disc type tribometer (DUCOM, TL-20, Bangalore, India) with data acquisition system was used to measure the wear friction behaviour of FGMs and base alloys against high-carbon chromium steel disc (HRC-64) as counter surfaces having surface roughness ( $R_a$ ) 0.5m as shown in Fig.4. Cylindrical wear samples of 30 mm length and 8 mm diameter were used for wear and friction tests against a hardened steel disc. Wear tests were carried out at four different loads 10, 20, 30 and 40 N for a fixed sliding velocity of 2.15 m/s for a total sliding distance of about 3000 metres. In this study, all tests were performed at room temperature under dry sliding conditions. During the wear test experiment, the pin samples were ultrasonically

cleaned with acetone after each test and weight loss was measured with a digital balance with least count of 0.1 mg. Wear rate was calculated from the weight loss measurements. Coefficient of friction was determined from the applied load and frictional force. Ratio of frictional force to applied load gives the data of coefficient of friction. Three samples were tested at each condition and average value is reported.

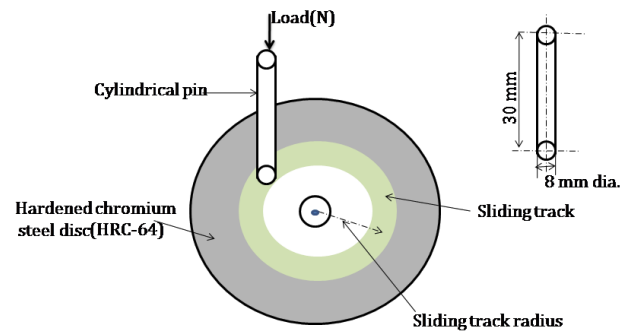


**Fig. 4.** Schematic illustration of pin-on-disc type tribometer.

### 3. RESULTS AND DISCUSSION

#### 3.1 XRD analysis

Figure 5 shows the XRD patterns of developed A356 alloy and in-situ fabricated composites with different composition 5, and 10 wt.% of Mg

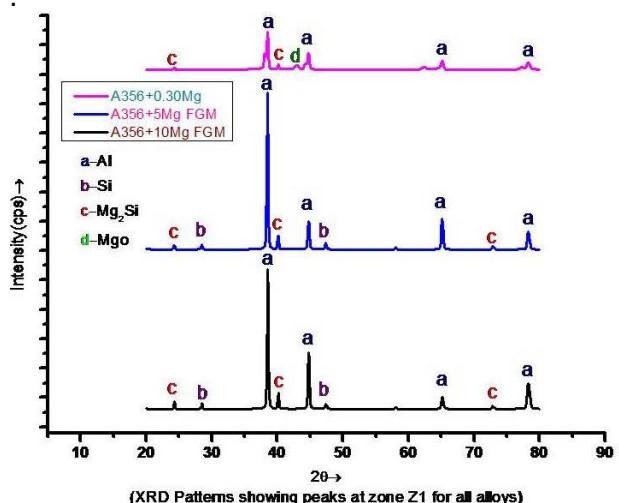


**Fig. 5.** XRD pattern showing the clear peaks of phase particles for each alloys (a) A356 Alloy, (b) A356+5Mg at 1200 rpm and (c) A356+10Mg at 1600 rpm.

Diffraction peaks of  $Mg_2Si$  particles were clearly seen for all compositions which confirm the presence of in-situ formed  $Mg_2Si$  particles into inner core of cast tubular products. It was also

observed that intensity of the Mg<sub>2</sub>Si diffraction peaks increases with increasing the Mg amount and fraction of Mg<sub>2</sub>Si primary particles.

### 3.2. Microstructural Characterization

The gradient structures of FGMs are observed at different rotational speeds of the mould and due to the action of centrifugal force. In fact, primary reinforcing phase Mg<sub>2</sub>Si have lighter density than matrix are migrated into inner zone Z<sub>1</sub>, but due to faster cooling rate some particles are settled at periphery Z<sub>3</sub> and provide the thermal stability along the thickness [17,20-21]. So, at initial mould temperature (room temperature) many particles can leads to a smaller grain size and the phase constitution along the radius, no significant differences were detected in zone Z<sub>3</sub>. Regarding Mg<sub>2</sub>Si particles content, a gradient structure was also obtained in the both 5 wt.% Mg and 10 wt.% Mg samples, as expressed by Fig. 6 and particles were distribution of the Mg<sub>2</sub>Si particles fraction area as a function of the distance to the geometrical centre of the ring is presented.

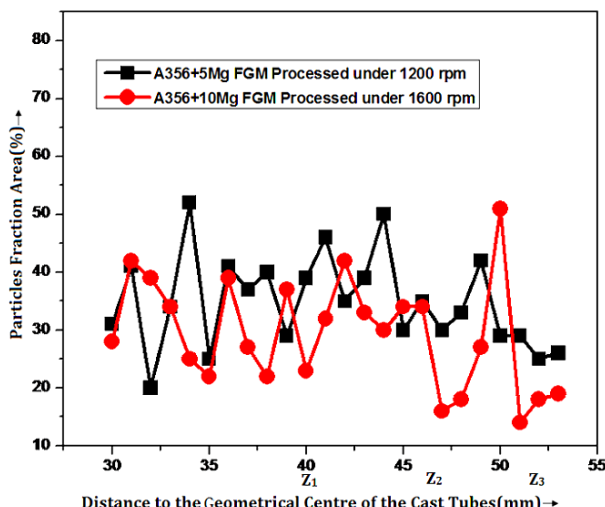


Fig. 6. Distribution of the Mg<sub>2</sub>Si particles fraction area as a function of the distance to the geometrical centre for both FGM's cast at 1200 and 1600 rpm.

SEM micrographs of the centrifugally cast in-situ composites with variations of Mg Contents are presented by Fig. 7(a) A356+5Mg and 7(b) A356+10Mg FGMs processes under 1200 rpm and 1600 rpm respectively at: inner zone Z<sub>1</sub> of the rings. Analysis made on centrifugally cast FGM's; some porosity is observed into the inner zone of the tubes at zone Z<sub>1</sub>. These defects are being more pronounced in the centrifugal casting at lower rotation speeds.

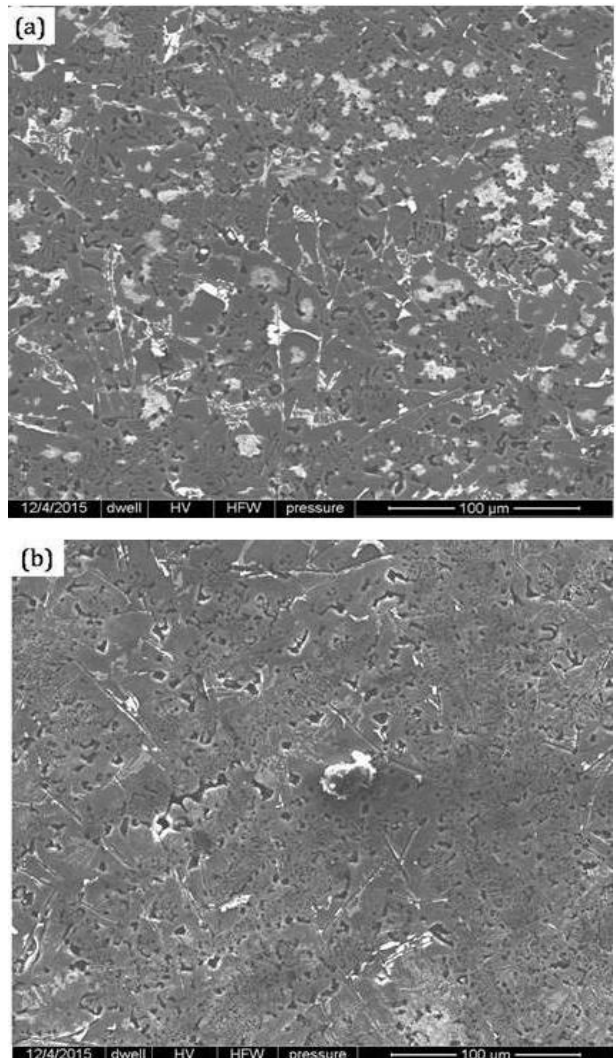
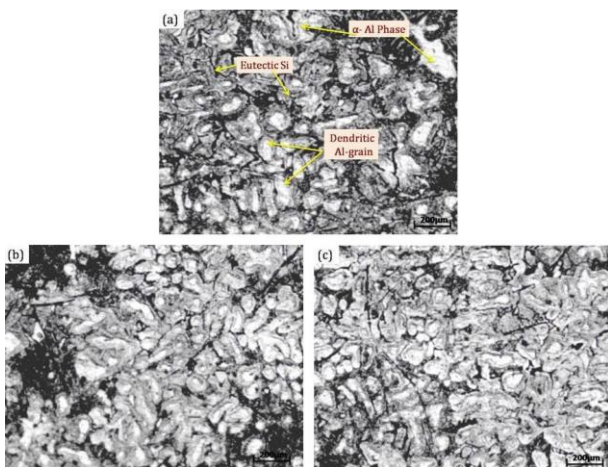


Fig. 7. SEM micrographs of the centrifugally cast FGMs (a) A356+5Mg processes under 1200 rpm and (b) A356+10Mg FGMs processes under 1600 rpm observed at: inner zone Z<sub>1</sub> of the rings.

For FGM processed at 1200 rpm, a monotonically variation in the amount of particles occurs from the outer (Z<sub>3</sub>) to the inner part (Z<sub>1</sub>) of the ring, resulting in a very low number of particles presented in zone Z<sub>2</sub> and negligible at Z<sub>3</sub>. However, higher centrifugal speed results in a more gathering of Mg<sub>2</sub>Si particles into inner core of the ring and achieved more hardness and wear resistance properties. This variation of the amount of particles in the matrix from outer zone to inner layer depends on the rotational speed of the mould. Consequently, in zone Z<sub>3</sub> the amount of reinforcing particles is higher for FGM processed under 1200 rpm, while the opposite occurs in zone Z<sub>2</sub>. Similarly for FGM processed under 1600 rpm, the variation of particles distributions and gradient properties enhanced at Z<sub>1</sub> than Z<sub>3</sub>. In both

FGM at 1200 rpm and FGM at 1600 rpm, the zone  $Z_3$  is almost completely depleted of  $Mg_2Si$  particles.



**Fig. 8.** Optical micrographs of the A356 alloy processed under 1200 rpm at (a) Inner zone  $Z_1$ , (b) Middle Zone  $Z_2$  and (c) outer zone  $Z_3$ .

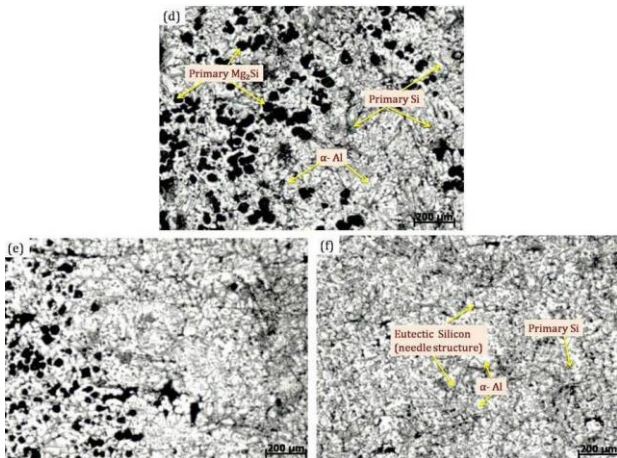


**Fig. 9.** Optical micrographs of the A356+5Mg FGM's processed under 1200 rpm at (d) Inner zone  $Z_1$ , (e) Middle Zone  $Z_2$  and (f) outer zone  $Z_3$ .

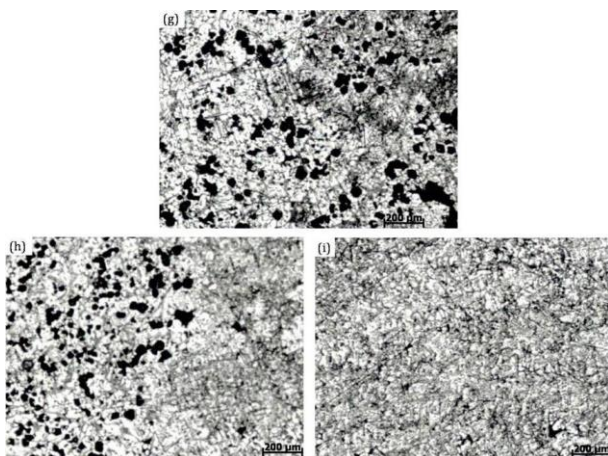


**Fig. 10.** Optical micrographs of the A356+10Mg FGM's processed under 1600 rpm at (g) Inner zone  $Z_1$ , (h) Middle Zone  $Z_2$  and (i) outer zone  $Z_3$  from geometrical centre of tubes.

The optical micrographs were taken to reveals the microstructures of the centrifugally cast A356 alloy and of both FGMS, in the different zones at inner ( $Z_1$ ), middle ( $Z_2$ ) and outer ( $Z_3$ ) in this study and presented by in Figs. 8, 9 and 10, respectively.

### 3.3. Hardness result

The evolution of the distribution of  $Mg_2Si$  particles had a significant effect in terms of hardness as shown in Fig. 11. As resultant the hardness is more at zone  $Z_1$  but gradually decreases zone  $Z_2$  to zone  $Z_3$  was observed for all materials, this effect being much more pronounced due to particles segregation in the case of FGM composites. For the centrifugally cast of A356 alloy, the smooth variation in hardness is observed mainly due to absence of reinforcement particles and microstructure is un-effected with grain size.

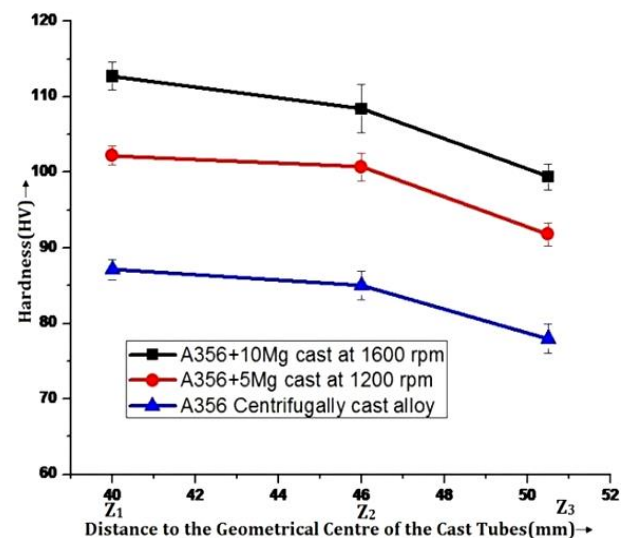


**Fig. 11.** Hardness evolution as function of the distance to the geometrical centre of the FGM tube for both FGM's cast at 1200 and 1600 rpm and A356 alloy cast at 1200 rpm.

### 3.4. Wear Behaviour

Metal matrix composites have found application in the manufacture of various fields especially in automotive engine components such as cylinder blocks, pistons and liners where adhesive wear (or dry sliding wear) is a predominant process. When materials possessing under dry sliding conditions then high wear resistance are associated with a stable tribolayer on the wearing surface and the formation of equiaxed or fine wear debris. For dry sliding wear, the

influence of load, sliding speed, wearing surface hardness, reinforcement fracture toughness and morphology are several critical parameters in relation to the wear regime encountered by the material. The effect of various wear parameters such as sliding distance, applied load and weight percentages of Mg contents on wear and friction behaviour of composites has been discussed in the following sections.

### 3.4.1 Effect of sliding distance

Figure 12 (a) represents the variation of cumulative weight loss of A356 alloy and composites as a function of sliding distance at 40N load and sliding velocity 2.15 m/s. It is observed that weight loss increases with increasing the sliding distance for all composites and base alloy. However, a decrease in wear loss is observed with increasing weight fraction of Mg<sub>2</sub>Si particles with respect to increasing Mg contents.

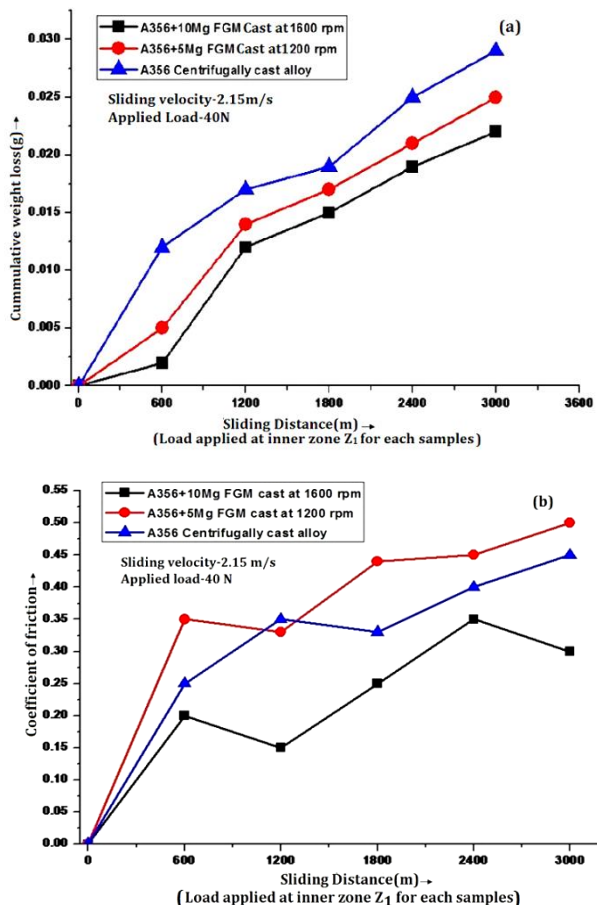


**Fig. 12.** Variation of (a) cumulative wt. loss and (b) COF with sliding distance(m) at zone Z<sub>1</sub>(inner core) to the geometrical centre of the FGM tube for both FGM's cast at 1200 and 1600 rpm and A356 alloy cast at 1200 rpm.

It is also observed from Fig. 12 (a) that cumulative wear rate increases after sliding a distance of 2400 m and 3000 m which may be due to the distortion of surface with sliding distance. Figure 12 (b) shows the variation of the coefficient of friction (COF) with the sliding distance under dry sliding conditions at 40N normal load and for 2.15 m/s sliding velocity with different wt.% of Mg<sub>2</sub>Si. Coefficient of friction of composites is higher than base alloy while sliding under identical conditions.

The higher coefficients of friction in the case of composites are due to the presence of hard particles at the interface between two contacting surfaces. When the effective load is above of its flexural strength, the particles get fractured and entrapped within the softer surface and coefficient of friction fluctuates within a value of  $\pm 0.020$  to  $\pm 0.030$ .

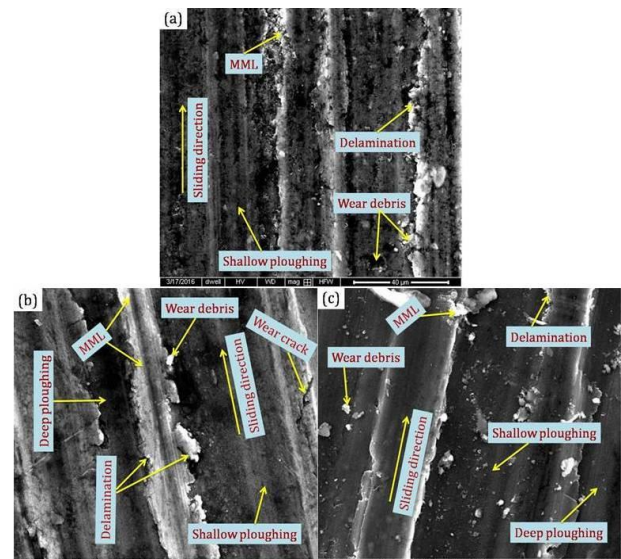


**Fig. 13.** SEM micrographs of worn surfaces at constant load (40 N) for (a) A356 alloy, (b) A356+5Mg FGM and(c) A356+10Mg FGM at Z<sub>1</sub>.

Fig.13 (a), (b) and (c) reveal the morphology of the worn surfaces of A356 alloy and cast FGMs at 2.15 m/s sliding velocity and 40 N load after sliding distances at 1200 m, 2400 m and 3000m. Figure 13 (a) reveal the shallow ploughing marks and grooves, delamination is observed at 1200 m whereas in Fig. 13 (b) and (c) deep ploughing and grooves with high degree of delamination are visible after sliding distance of 2400 m and 3000 m with some wear cracks were also observed.

### 3.4.2 Effect of applied load

It is evident from Fig.14 (a), that wear rate increases with increase in applied load for both centrifugally cast A356 alloy as well as FGMs. At low loads wear rate increases linearly but after 30 N load transitions in wear behaviour takes place from mild to severe and a sudden increase in wear rate is observed.

The reason for increased wear rate may be due increases in contact area between the two surfaces with increase in load, which leads to generation of high amount of frictional heat between the surfaces. High frictional heating results in softening of the pin surface and increased wear rate due to more penetration of hard asperities into soft pin surface. The increase in the applied load may also lead to increase in micro cracking tendency of the subsurface as well as deformation and fracture of asperities. These asperities are either removed from the surface or deformed in the sub-surface.

In the presence of hard primary Mg<sub>2</sub>Si particles a mechanically mixed layer (MML) of soft aluminum base matrix and hard particles of Mg<sub>2</sub>Si is formed (Figs. 15a and b). At low loads this MML restricts the transfer of material from the surface and the wear rate is less, or it is in mild wear regime and oxidative wear dominates. But, after a transition load of 30N cracking of this MML takes place and hard Mg<sub>2</sub>Si particles come out (Fig. 15c) and act as third body abrasion and wear mechanism changes from mild to severe giving rise to oxidative metallic wear as observed in Fig. 14a, and the wear rate increases.

At low loads wear surface morphology exhibits relatively smooth areas with shallow grooves, (Fig. 15a and b) but as the load increases MML is broken, and wear surface exhibits deep grooves, severely damaged areas, delamination and large number of cracks (Fig. 15c) which leads to the increased wear rate. Initially, coefficient of friction decreases with load up to 30 N but at higher load i.e. beyond 30N formation for larger small hard particles of Mg<sub>2</sub>Si in MML contributes to friction and it starts increasing with load (Fig. 14b).

### 3.4.2 Effect of constant load with variations of Mg content

Wear rate of the composites decreases with increase the Mg contents along with increase the particles at a constant sliding velocity of 2.15 m/s and at constant applied loads of 40 N as evident as shown in Fig. 16(a). This may be due to refinement of  $\alpha$ -Al grains and excellent interfacial bonding between the reinforced Mg<sub>2</sub>Si particles and matrix which enhance the load bearing capacity of composites [22].

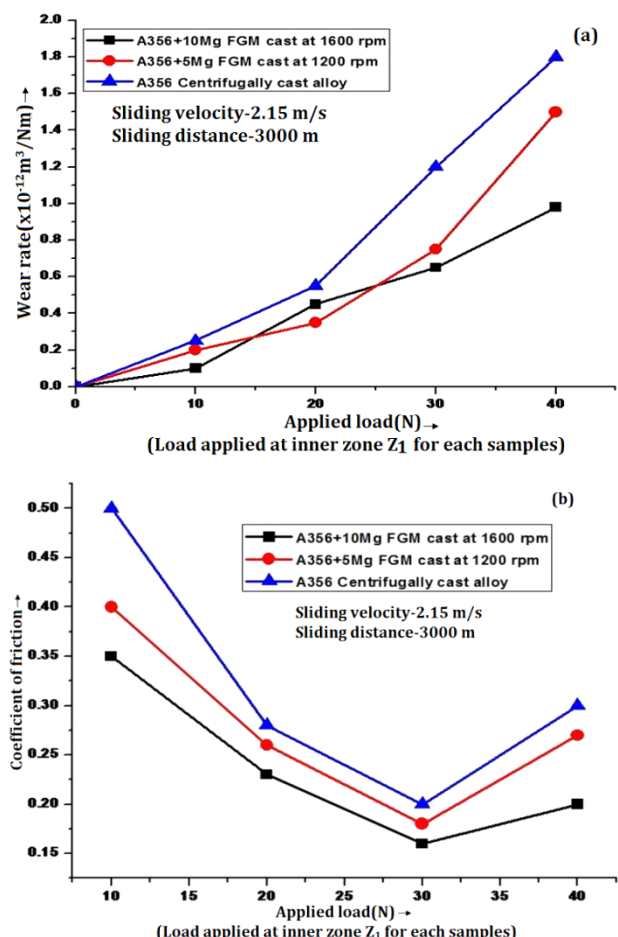


**Fig. 14.** (a) Variation of wear rate with applied load and (b) Variation of COF with applied load for both FGMs processed under 1200 rpm and 1600 rpm and A356 alloy processed under 1200 rpm.

It is also reported that more grain boundary per unit area of Al matrix is observed due to fine grain structure which enables to higher load bearing capacity and wear resistance as compared to the coarse grain structure [23]. Also in addition, Mg<sub>2</sub>Si particles reduce the extent of direct metal-to-metal contact between matrix and counterpart, thus, Mg<sub>2</sub>Si particles act as a load bearing phase and protects the matrix during sliding process.

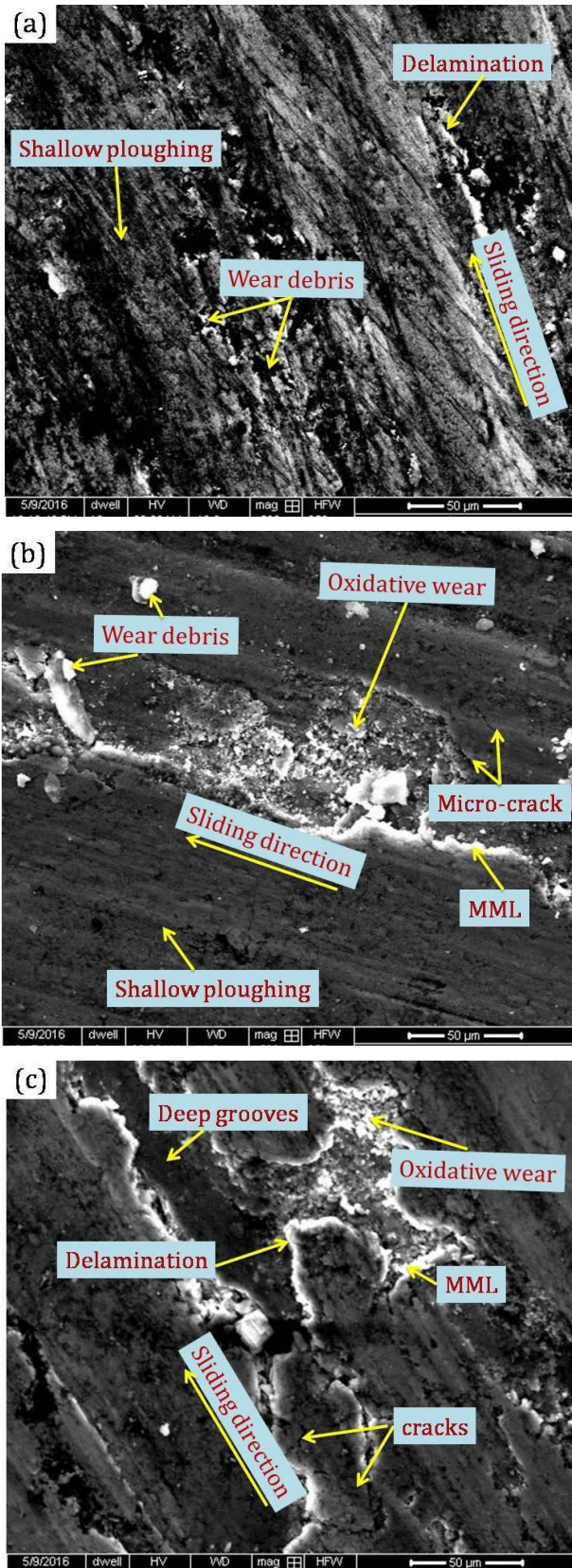


**Fig. 15.** SEM micrographs of worn surfaces with load variations (a) A356 alloy, (b) A356+5Mg FGM and(c) A356+10Mg FGM at  $Z_1$ .

As increase in the Mg content more formation of  $Mg_2Si$  particles results in an increase in

dislocation density around the  $Mg_2Si$  particles during solidification hence, strength and hardness of composites improve which contributes to lower the wear rate [24]. Further, increase in percentage of  $Mg_2Si$  in MML also restricts the removal of material from the surface due to increased hardness of composite and wear rate decreases which is in agreement with Archard's wear law [25]. Hence, wear rate of composites reduces with the content of  $Mg_2Si$ . It was observed that, the increase in hardness due to the refinement of grain structure, reinforcement of hard in-situ formed  $Mg_2Si$  particles, presence of MML and good interfacial bonding.

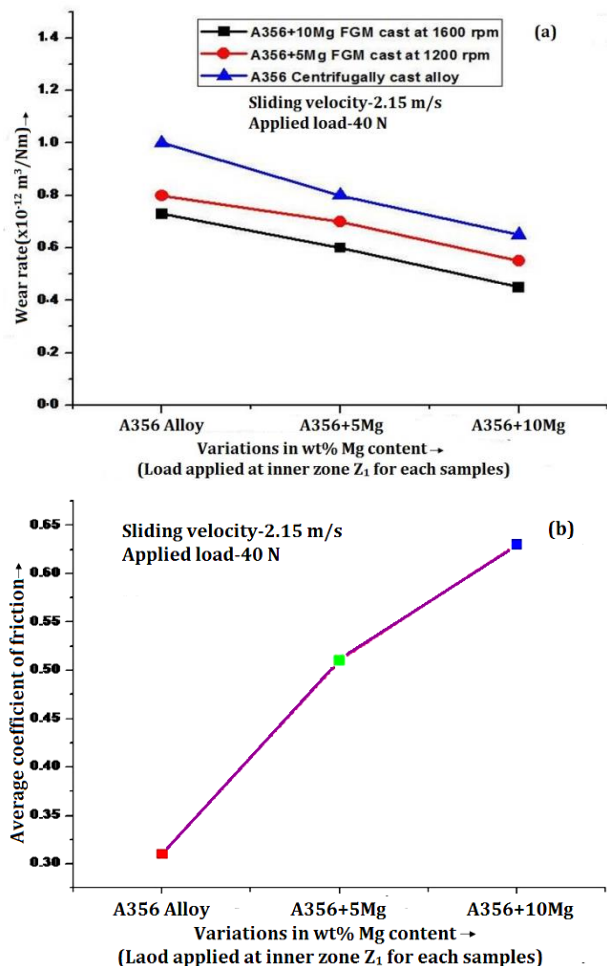


**Fig. 16.** Effect of constant load on (a) wear rate (b) average COF with variations of Mg contents.

Figure 16 (b) shows the variation of average coefficient of friction with wt.% of Mg along the  $Mg_2Si$  particles at 40 N applied load and sliding velocity 2.15 m/s. It is observed that coefficient of friction increases with increasing the vol.%  $Mg_2Si$  particles. With increase in the amount of  $Mg_2Si$  particles in the MML total coefficient of

friction increase as a result of increased presence of large abrasive particles where as other factors contributing to friction remain more or less, and therefore continuous increase in coefficient of friction is observed.

### 3.5. Characterization of the worn surfaces

Aluminium, Magnesium and traces of Fe were detected by EDS analysis in the wear track of inner zone Z<sub>1</sub> of FGM processed at 1600 rpm (Fig. 17(a) & (b)). This EDS observation confirms the presence of particles and also an oxidative wear mechanism. In EDS analysis, the presence of oxidized material that suggests the formation of the formation of a mechanically mixed layer (MML) and an oxide tribolayer.

The formation of MML by transfer of material between the mating surfaces, the existence of fragments of oxide material and/or oxide layers and compaction of these fragments on the surface is observed. Delaminating of the MML often suggest, the formation of this layer and continuous destruction of material on the wear track may occurred. Also, the load-bearing action of the reinforced primary Mg<sub>2</sub>Si particles can help the subsequent formation of MML and accommodation of material.

EDS analysis of these darker areas revealed a high oxygen content, which suggests the occurrence of strong oxidation due to relatively high temperatures developed during the sliding process. At higher magnification (Fig. 17(b)), the presence of plastic deformation and oxygen-rich tribolayers is evidenced. Corroborating these results, the morphological characteristics of loose wear debris (Fig. 15(c)) denote a plate-like and ribbon shape, which is typically found in the presence of a severe wear regime.

This relation between both EDS observation morphological features and wear coefficient values obtained for the centrifugally cast Al alloy agrees with the concept of severe wear regime [26].

Part of the oxidized material transferred to the steel surface is removed during the sliding process and could appears to the surface of Al matrix as an agglomerate of transferred material, whereas the re-oxidation is occurs of "new clean" steel surface.

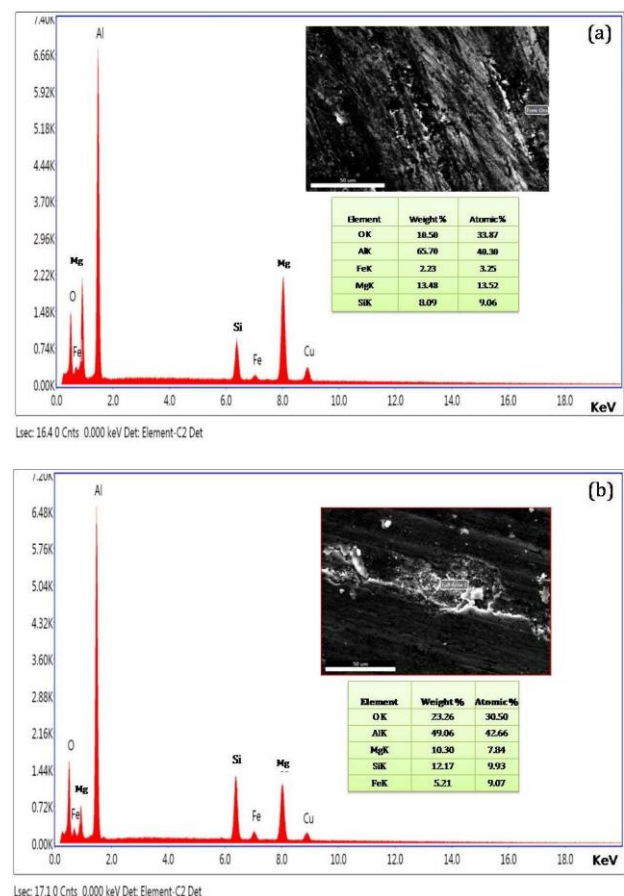


**Fig. 17.** SEM morphology of wear surface at load 40N and EDS spectrum for both FGMs (a)A356+5Mg processed under 1200rpm (b)A356+10Mg processed under 1600 rpm at inner zone Z<sub>1</sub> of geometrical tube.

In periphery at zone Z<sub>3</sub> (outer) of both FGMs, represent depleted zone of the Mg<sub>2</sub>Si particles, similar results in the case of centrifugally cast A356 alloy were obtained. The presence of tribolayers in the wear track generated during the sliding processes plate-like and ribbon shapes characterizing the morphology of loose wear debris and transfer of Al-based material from FGM tubes to the steel counter surfaces by adhesion. Thus, a severe wear regime also occurred in zone Z<sub>3</sub> of FGM rings. Although in zone Z<sub>2</sub> of FGM processed under 1200 rpm the Mg<sub>2</sub>Si area fraction is of about 2.3 %, no significant change on wear behaviour was reported.

However, considering zone Z<sub>2</sub> of FGM processed under 1600 rpm, where the Mg<sub>2</sub>Si fraction area is of 6.5% but some differences start to appear. Moreover, it can be suggested that at the intermediate wear regime between mild wear and severe wear occurs for the amount of reinforcing particles corresponding to zone Z<sub>2</sub> of fabricated FGMs processed under 1600 rpm.

The effect of a higher content of reinforcing particles can be seen by the morphological features and EDS data presented in Fig. 17 (a) and (b) corresponding to a wear test in zone Z<sub>1</sub> of the FGM composite cast at 1200rpm (~46 % Mg<sub>2</sub>Si), which are also representative of the results obtained with 1600 rpm FGM composite in zone Z1 (~60-65 % Mg<sub>2</sub>Si).

The SEM micrograph of the composite worn surface presented in Fig. 15 (b) and (c) shows the several tribolayers at protruding Mg<sub>2</sub>Si particles and some delamination of that tribolayers was observed. The presence of protruding reinforcing Mg<sub>2</sub>Si particles at the composite worn surface shows the existence of a strong interfacial bonding between reinforcement and matrix [15]. It is known that hard Mg<sub>2</sub>Si particles act as load-bearing elements in Al-(Mg<sub>2</sub>Si)p composites, promoting the formation and stability of adherent thick tribolayers. This process is known to be determinant to improve the wear resistance of the composites.

## 4. DISCUSSION

### 4.1 Effect of varying mold rotational speed

It was found that in Al-Mg<sub>2</sub>Si composites the Si and Mg<sub>2</sub>Si primary particles are formed and migrate into inner core. The alloys were abundantly segregated and enriched in the inner layer of castings in the centrifugal field due to their smaller densities ( $\rho_{\text{Si}} = 2.33 \text{ g/cm}^3$ ,  $\rho_{\text{Mg}_2\text{Si}} = 1.99 \text{ g/cm}^3$ ) than that of Al melt ( $\rho_{\text{Al}} = 2.37 \text{ g/cm}^3$ ). Primary Si and Mg<sub>2</sub>Si were gathered in the inner layer few of them gathered in the middle layer which will depends on rotational speed and density of particles [27].

### 4.2 Effects of mold temperature

Changming Liu et al. were studied that, when higher the mould temperature, then longer the solidification time of molten metal; therefore, when the mould temperature was high, there is enough time for primary silicon and Mg<sub>2</sub>Si grains to be gathered to the inner layer under a certain centrifugal force. However, when the mould temperature was low, there is not enough time for primary silicon and Mg<sub>2</sub>Si grains to be gathered to the inner layer, so fewer primary

silicon and Mg<sub>2</sub>Si grains were gathered in the inner layer. In the outer layer Zone Z<sub>3</sub>, the mould temperature was low and the degree of under cooling was high, the nucleation of particles was easy. Therefore, a few primary Si and Mg<sub>2</sub>Si particles were gathered in the outer layer.

### 4.3 Effects of pouring temperature

Usually, when the pouring temperature is high, the degree of superheat of the molten alloy is also higher; therefore, the cooling rate of castings is slow but period of solidification time is longer. This long period of cooling time may provide the more gathering of particles grains under a centrifugal force. When the pouring temperature is high, primary silicon and Mg<sub>2</sub>Si grains were gathered more obviously in the inner layer. However, when the pouring temperature is too high, the primary Mg<sub>2</sub>Si and Si would be coarse grains because of the high degree of superheat in the melt and the long period of solidification take place. Therefore, the pouring temperature should be carefully controlled at a suitable temperature range [27].

### 4.4 Effects of G -Factor

As shown in Fig. 18 of microstructure the primary Mg<sub>2</sub>Si/Si particles were distributed and migrated into inner or outer periphery which is generally depends on G-Factor or number. The gradient segregation of particles is observed because of due to action of centrifugal force. Generally, it is the ratio of centrifugal force to gravitational force and expressed as follows.

$$G = \frac{\omega r^2}{g}$$

where r is radius of cast tube and  $\omega$  is angular velocity (radian.s<sup>-1</sup>).

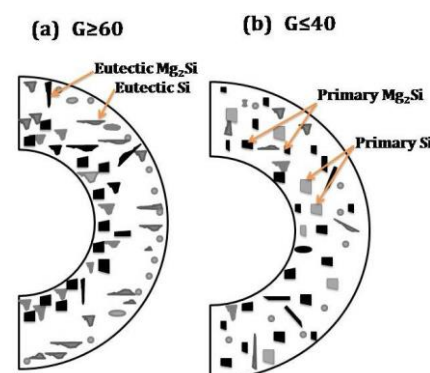


**Fig. 18.** Particles segregation mechanisms under effect of G-Factor.

When the pouring temperature was 720 °C and mold temperature was 90 °C, as G≥60, many particles migrated into the inner layer, and the reinforcement layer will form, but when G≤40, the reinforcement layer could not be formed and the particles are distributed throughout the whole cross section of cast tubes [27].

#### 4.5 Effects of varying Si content

Silicon is a major alloying element in the most of the common aluminum casting alloys and it provides the excellent of fluidity and flowability. Therefore, Al-Si alloys have a good combination of mechanical properties and castability. Moreover, they are widely used in the automotive, aerospace industry and casting industries. Silicon increases the fluidity in aluminum casting alloys and reduces the hot tears tendencies and solidification interval [28].

#### 4.6 Effects of varying Mg content

The coefficient of thermal expansion and its electrical resistivity are decreases when increases the Mg. Aluminum-magnesium alloys have high strength, good ductility and excellent corrosion resistance. Aluminum-magnesium alloys respond well on heat treatment and a higher ultimate tensile strength and yield strength is achieved. The purposes of magnesium in Al-Si alloys are to precipitate Mg<sub>2</sub>Si particles but a disadvantage is that big intermetallic compounds can appear; those phases reduce the ductility. In alloys that have an amount of magnesium between 0.05 % to 0.3 % seems to decrease the amount of porosity [29].

### 5. CONCLUSIONS

The dry sliding wear behaviour of centrifuged Al alloy and Al-Mg<sub>2</sub>Si<sub>p</sub> FGMMC's processed with different centrifugal speeds was studied by Pin-on-Disc tribometer using high-carbon chromium steel (HRC-64) as counter surface. The following conclusions can be stated:

1. Apart from several processing techniques of FGMs, the centrifugal casting technique has a unique characteristic to promote a gradient in the microstructure and in hardness of the centrifugally cast Al-Si alloy due to differences of cooling rates. The cast

functionally graded material was characterized by severe wear assisted by an adhesive wear mechanism.

2. According to observations, FGM produced at low centrifugal speed (1200 rpm) showed a smooth gradient of Mg<sub>2</sub>Si phase distribution, while FGM produced at higher centrifugal speed (1600 rpm) revealed a very sharp graded on the distribution of reinforcing phase particles. This gradient was controlled by the movement of the solidification front, blocking the mobility of Mg<sub>2</sub>Si particles in the melt.
3. A relation between the wear coefficient and the relative area fraction of Mg<sub>2</sub>Si particles was found: the increase of Mg content resulted in a fast decrease of the FGM composite wear coefficient, followed by increase in Mg<sub>2</sub>Si particles but much low Mg content, decrease of the wear coefficient values with the incorporation of Mg<sub>2</sub>Si particles above 10 %. Also, a relation was found between the amount of Mg<sub>2</sub>Si reinforcing particles and the type of wear regime. For Mg<sub>2</sub>Si contents lower than~5 % the severe wear regime was dominant, followed by a continuous transition to a mild wear regime when the highest content of Mg<sub>2</sub>Si p is attained (~47 %).

### Acknowledgement

The research was financially supported by the MHRD Government of India, under Research support grant to faculty (RSGF) scheme, Department of Metallurgical Engineering IIT(BHU),Varanasi-UP (India)-221005.

### REFERENCES

- [1] A.I. Taub, P.E. Krajewski, A.A. Luo and J.N. Owens, 'The evolution of technology for materials processing over the last 50 years: The automotive example', *JOM.*, vol. 59,no. 2, pp. 48-57, 2007.
- [2] T. Zeuner and L. Wurker, 'Process optimisation of cast aluminium chassis components'. *HOMMES ET FONDERIE*, pp. 28-32, 2004.
- [3] Ye, Haizhi, 'An overview of the development of Al-Si-alloy based material for engine applications,'

- Journal of Materials Engineering and Performance*, vol. 12, no. 3, pp. 288-297, 2003.
- [4] S. Ji, D. Watson, Z. Fan and M. White, 'Development of a super ductile die cast Al-Mg-Si alloy', *Materials Science and Engineering: A*, vol. 556, pp. 824-833, 2012.
- [5] L. Wang, M. Makhlof and D. Apelian, 'Aluminium die casting alloys: alloy composition, microstructure, and properties-performance relationships', *International Materials Reviews*, vol. 40, no. 6, pp. 221-238, 1995.
- [6] V.S. Zolotorevsky, N.A. Belov and M.V. Glazoff, *Casting aluminum alloys*. Oxford: Elsevier, 2007.
- [7] M. Emamy, H.R.J. Nodooshan and A. Malekan, 'The microstructure, hardness and tensile properties of Al-15% Mg<sub>2</sub>Si in situ composite with yttrium addition', *Materials & Design*, vol. 32, no. 8, pp. 4559-4566, 2011.
- [8] M. Emamy, R. Khorshidi and A. Honarbakhsh Raouf, 'The influence of pure Na on the microstructure and tensile properties of Al-Mg<sub>2</sub>Si metal matrix composite', *Materials Science and Engineering: A*, vol. 528, no. 13, pp. 4337-4342, 2011.
- [9] M.R. Ghorbani, M. Emamy and N. Nemati, 'Microstructural and mechanical characterization of Al-15% Mg<sub>2</sub>Si composite containing chromium', *Materials & Design*, vol. 32, no. 8, pp. 4262-4269, 2011.
- [10] Y.-B. Zhai, C.-M. Liu, K. Wang, M.-H. Zou and Y. Xie, 'Characteristics of two Al based functionally gradient composites reinforced by primary Si particles and Si/in situ Mg<sub>2</sub>Si particles in centrifugal casting', *Transactions of Nonferrous Metals Society of China*, vol. 20, no. 3, pp. 361-370, 2010.
- [11] X. Lin, C. Liu, Y. Zhai and K. Wang, 'Influences of Si and Mg contents on microstructures of Al-xSi-yMg functionally gradient composites reinforced with in situ primary Si and Mg<sub>2</sub>Si particles by centrifugal casting', *Journal of Materials Science*, vol. 46, no. 4, pp. 1058-1075, 2011.
- [12] F. Gul and Mehmet Acilar, 'Effect of the reinforcement volume fraction on the dry sliding wear behaviour of Al-10Si/SiC p composites produced by vacuum infiltration technique', *Composites Science and Technology*, vol. 64, no. 13-14, pp. 1959-1970, 2004.
- [13] M. Acilar and F. Gul, 'Effect of the applied load, sliding distance and oxidation on the dry sliding wear behaviour of Al-10Si/SiCp composites produced by vacuum infiltration technique', *Materials & design*, vol. 25, no. 3, pp. 209-217, 2004.
- [14] D.P. Mondal, S. Das, R.N. Rao and M. Singh, 'Effect of SiC addition and running-in-wear on the sliding wear behaviour of Al-Zn-Mg aluminium alloy', *Materials Science and Engineering: A*, vol. 402, no. 1, pp. 307-319, 2005.
- [15] D.P. Mondal and S. Das, 'High stress abrasive wear behaviour of aluminium hard particle composites: Effect of experimental parameters, particle size and volume fraction', *Tribology international*, vol. 39, no. 6, pp. 470-478, 2006.
- [16] J.R. Gomes, A.S. Miranda, L.A. Rocha and R.F. Silva, 'Effect of Functionally Graded Properties on the Tribological Behaviour of Aluminium-Matrix Composites', *Key Engineering Materials*, vol. 230-232, pp. 271-274, 2002.
- [17] J.R. Gomes, L.A. Rocha, S.J. Crnkovic, R.F. Silva and A.S. Miranda, 'Friction and wear properties of functionally graded aluminum matrix composites', *Materials Science Forum, Trans Tech Publications*, vol. 423, pp. 91-96, 2003.
- [18] L. Zhang, X.B. He, X.H. Qu, B.H. Duan, X. Lu and M.L. Qin, 'Dry sliding wear properties of high volume fraction SiC p/Cu composites produced by pressureless infiltration', *Wear*, vol. 265, no. 11, pp. 1848-1856, 2008.
- [19] X.Y. Li and K.N. Tandon, 'Microstructural characterization of mechanically mixed layer and wear debris in sliding wear of an Al alloy and an Al based composite', *Wear*, vol. 245, no. 1, pp. 148-161, 2000.
- [20] A.C. Vieira, P.D. Sequeira, J.R. Gomes and L.A. Rocha, 'Dry sliding wear of Al alloy/SiCp functionally graded composites: Influence of processing conditions', *Wear*, vol. 267, no. 1, pp. 585-592, 2009.
- [21] R. Asthana, 'Reinforced cast metals: Part I Solidification microstructure', *Journal of Materials Science*, vol. 33, no. 7, pp. 1679-1698, 1998.
- [22] C.S. Ramesh and A. Ahamed, 'Friction and wear behaviour of cast Al 6063 based in situ metal matrix composites', *Wear*, vol. 271, no. 9, pp. 1928-1939, 2011.
- [23] A.P. Rao, K. Das, B.S. Murty and M. Chakraborty, 'Effect of grain refinement on wear properties of Al and Al-7Si alloy', *Wear*, vol. 257, no. 1, pp. 148-153, 2004.
- [24] M. Gupta and T.S. Srivatsan, 'Interrelationship between matrix microhardness and ultimate tensile strength of discontinuous particulate-reinforced aluminum alloy composites', *Materials Letters*, vol. 51, no. 3, pp. 255-261, 2001.
- [25] J. Archard, 'Contact and rubbing of flat surfaces', *Journal of applied physics*, vol. 24, no. 8, pp. 981-988, 1953.

- [26] I.M. Hutchings and P. Shipway, *Tribology: friction and wear of engineering materials*. Butterworth-Heinemann, 1992.
- [27] X. Lin, C. Liu and H. Xiao, 'Fabrication of Al-Si-Mg functionally graded materials tube reinforced with in situ Si/Mg<sub>2</sub>Si particles by centrifugal casting', *Composites Part B: Engineering*, vol. 45, no. 1, pp. 8-21, 2013.
- [28] S. Spigarelli, E. Evangelista and S. Cucchieri, 'Analysis of the creep response of an Al-17Si-4Cu-0.55 Mg alloy', *Materials Science and Engineering: A*, vol. 387, pp. 702-705, 2004.
- [29] Y. Watanabe and H. Sato, 'Review Fabrication of Functionally Graded Materials under a Centrifugal Force,' INTECH Open Access Publisher, DOI: 10.5772/20988, pp. 133-150, 2011.